



Water Resources Research

RESEARCH ARTICLE

10.1029/2020WR027306

Special Section:

Coastal hydrology and oceanography

Key Points:

- Transport of particulate organic carbon (POC) creates carbon pools dependent on flow conditions and aquifer properties
- POC contribution to aquifer biogeochemistry is dependent on hydrologic transience and factors that increase POC overlap with reactive solutes
- Transient POC pools support intermittent hot spots of denitrification, creating a “carbon memory” effect

Supporting Information:

- Supporting Information S1

Correspondence to:

H. A. Michael,
hmichael@udel.edu

Citation:

Kim, K. H., Heiss, J. W., Geng, X., & Michael, H. A. (2020). Modeling hydrologic controls on particulate organic carbon contributions to beach aquifer biogeochemical reactivity. *Water Resources Research*, 56, e2020WR027306. <https://doi.org/10.1029/2020WR027306>

Received 11 FEB 2020

Accepted 31 AUG 2020

Accepted article online 9 SEP 2020

Modeling Hydrologic Controls on Particulate Organic Carbon Contributions to Beach Aquifer Biogeochemical Reactivity

Kyra H. Kim^{1,2} , James W. Heiss³ , Xiaolong Geng¹ , and Holly A. Michael^{1,4} 

¹Department of Earth Sciences, University of Delaware, Newark, DE, USA, ²School of Marine Science and Policy, University of Delaware, Newark, DE, USA, ³Department of Environmental, Earth and Atmospheric Sciences, University of Massachusetts Lowell, Lowell, USA, ⁴Department of Civil and Environmental Engineering, University of Delaware, Newark, DE, USA

Abstract The intertidal zone of beach aquifers hosts biogeochemical transformations of terrestrially derived nutrients that are mediated by reactive organic carbon from seawater infiltration. While dissolved organic carbon is often assumed the sole reactive organic carbon component, advected and entrapped particulate organic carbon (POC) is also capable of supporting chemical reactions. Retarded advection of POC relative to groundwater flow forms pools of reactive carbon within beach sediments that support biogeochemical reactions as dissolved solutes move across them due to transient groundwater flow. In this work, we simulate the contribution of POC to beach reactions and identify parameters that control its relative contribution using a groundwater flow model (SEAWAT) and reactive transport model (PHT3D). Results show transient contributions of POC to denitrification, as the spatial extent of the saline circulation cell varies over time due to changing hydrologic factors. A decrease in POC retardation and an increase in tidal amplitude during POC deposition resulted in POC expansion, which increased the relative contributions of POC to beach reactivity. Decreased hydraulic conductivity and increased tidal amplitude post-deposition decreased the utilization of POC for denitrification by allowing the oxic, saline water to completely encompass the pool of POC. Results highlight that POC is an intermittently utilized source of carbon that displays complex spatial relationships with groundwater flow conditions and overall beach biogeochemistry. This work demonstrates that POC may be a periodically important but overlooked contributor to biogeochemical reactions in carbon-poor beach aquifers.

Plain Language Summary Sandy beaches are highly dynamic zones of fresh groundwater and seawater mixing. The mixing of the two waters allow chemical reactions that have the potential to directly influence the health of coastal ecosystems. One of the key reactants in these settings is organic carbon. Seawater often carries both dissolved and particulate organic carbon (POC), the latter often in the form of phytoplankton or algae. As seawater travels up the beach during waves and tides, the POC is delivered and deposited into the sands. However, due to its particulate form, it travels slower than dissolved organic carbon and lingers within the sands. These pools of POC then become potential reactors that are only utilized when other dissolved reactants are in contact. In this study, we identified the settings that promote the use of POC in beach reactions using a numerical model. Conditions that allowed for a larger POC extent, such as higher tides during POC delivery, allowed for more POC contributions of beach reactions. As the patterns of mixing between fresh water and seawater changed with spring and neap tides, the contributions of POC to beach reaction also changed over time, contingent on its contact with reactants from fresh water. Therefore, tide conditions that allowed for larger spatial overlap with POC and fresh water also served to increase reactions within the beach. Understanding the interactions between POC and water mixing within the beach is a key step to understanding beach reactions, which ultimately helps us better manage our marine environments.

1. Introduction

Coastal environments are ecologically, commercially, and recreationally valuable areas, supporting marine organisms, local fisheries, and tourism industries (Carter, 1988; Martínez et al., 2007). However, due to changes in land use and increased human activities in coastal areas, these systems are under threat

(Burak et al., 2004; Doney, 2010; Michael et al., 2017; Valiela et al., 1990). Increased fluxes of terrestrial nutrients to the ocean have caused adverse effects in coastal areas, including eutrophication, harmful algal blooms, and habitat losses (Andersen et al., 2007; Cloern, 2001; Diaz & Solow, 1999; Valiela et al., 1990; Vitousek et al., 1997). Ecosystem degradation further induces economic damage by influencing human health, tourism, and the fishing industry (Carter, 1988; Costanza et al., 1997; Martinez et al., 2007; van der Meulen et al., 2004). Therefore, understanding and managing terrestrial nutrient fluxes to marine systems is a critical aspect in the preservation of coastal environments.

Biogeochemical activity in coastal aquifers controls solute and nutrient fluxes to the adjacent marine system (Heiss et al., 2017; Kim et al., 2017, 2019; Slomp & Van Cappellen, 2004; Valiela et al., 1990). Terrestrial nutrients are delivered to beach sediments and ultimately to adjacent marine systems by fresh submarine groundwater discharge (SGD) (Johannes, 1980; Moore, 1999; Slomp & Van Cappellen, 2004; Valiela et al., 1990). During wave and tide activity, seawater travels up the beachface and infiltrates into the aquifer, overtaking seaward flowing fresh groundwater (Abarca et al., 2013; Michael et al., 2005; Robinson et al., 2006). The mixing between fresh groundwater and saline seawater creates a saltwater circulation cell in the intertidal zone (Heiss & Michael, 2014; Michael et al., 2005; Robinson et al., 2006; Vandebroek & Lebbe, 2006), which hosts dynamic biogeochemical reactions (Hays & Ullman, 2007; Kim et al., 2017, 2019; Slomp & Van Cappellen, 2004; Spiteri, Slomp, Tuncay, & Meile, 2008; Ullman et al., 2003). Fresh groundwater delivers terrestrial nutrients such as nitrate to the beach aquifer, which can be utilized as an alternative electron acceptor after oxygen depletion. Seawater delivers oxygen and reactive organic carbon to intertidal sediments. Various reactions including aerobic respiration (Anschtz et al., 2009; Charbonnier et al., 2013; Seidel et al., 2015), denitrification (Jiao et al., 2018; Kroeger et al., 2006; Kroeger & Charette, 2008; Lamontagne et al., 2018), and metal transformations (Charette & Sholkovitz, 2002; McAllister et al., 2015; Roy et al., 2010) have been observed in intertidal aquifers, impacting concentrations of solutes discharging to the coastal ocean.

In carbon-poor beach aquifer systems, the influx of reactive organic carbon from seawater is a key supply of electron donors that support biogeochemical reactions down the redox gradient (Anschtz et al., 2009; Anwar et al., 2014; Charbonnier et al., 2013). However, much of this previous work has been focused on dissolved organic carbon (DOC) as the dominant form of carbon within beach sediments. Field studies often measure surface water or porewater DOC to quantify and characterize organic carbon supply into the system (Beck et al., 2007; Chaillou et al., 2016; Charbonnier et al., 2013; Kim et al., 2012, 2013; O'Connor et al., 2018; Oh et al., 2017; Reckhardt et al., 2015; Seidel et al., 2014, 2015), and numerical modeling studies use DOC associated with seawater infiltration to support reactions (Anwar et al., 2014; Bardini et al., 2012; Heiss et al., 2017; Spiteri, Slomp, Charette, et al., 2008; Spiteri, Slomp, Tuncay, & Meile, 2008). While particulate organic carbon (POC) has not been completely disregarded in field settings (Beck et al., 2017; Charbonnier et al., 2013; Kim et al., 2017, 2019; Reckhardt et al., 2015), especially in its association with metal oxides (Charette et al., 2005; Roy et al., 2010, 2013), to date, most of the focus has been on the distribution, supply, and molecular quality of DOC and how DOC relates to biogeochemical reactions within beach sediments (e.g., Seidel et al., 2015), with few studies considering in situ POC (e.g., Heiss, 2020).

Fine carbon particles suspended in seawater have been shown to enter permeable coastal shelf sediments (McLachlan et al., 1985; Bacon et al., 1994; Huettel & Rusch, 2000; Pilditch & Miller, 2006; Rusch & Huettel, 2000; Rusch et al., 2000) and contribute to biogeochemical reactions (Huettel et al., 2014; Huettel & Rusch, 2000; Kim et al., 2019; Rusch et al., 2000). Similarly, POC in seawater enters the beach aquifer with DOC as a result of seawater infiltration. Unlike DOC that is mobile, transport of POC suspended in porewater is subject to dynamic transport mechanisms including retardation relative to groundwater advection, entrapment, immobilization, and remobilization (El-Farhan et al., 2000; McDowell-Boyer et al., 1986; Pronk et al., 2009). In beach aquifers, such particulate transport dynamics and frequent shifts in hydrologic conditions result in a spatially variable distribution of POC across the beach aquifer (Figure 1a). Recent field investigations at Cape Shores, Lewes, DE, USA, showed that these pools of reactive POC, potentially from algal fragments, beach wrack, and seagrass, retarded in their movement relative to groundwater flow, are important sources of nutrients and biogeochemical reactivity to the adjacent porewater (Kim et al., 2019). Numerical models also suggest that dissolution of POC from buried wrack can serve as an important organic carbon source to fuel reactivity in the beach (Heiss, 2020). As hydrological conditions (freshwater flux, tidal amplitude, and storms) change and mobile reactants move across the pool of POC, favorability of

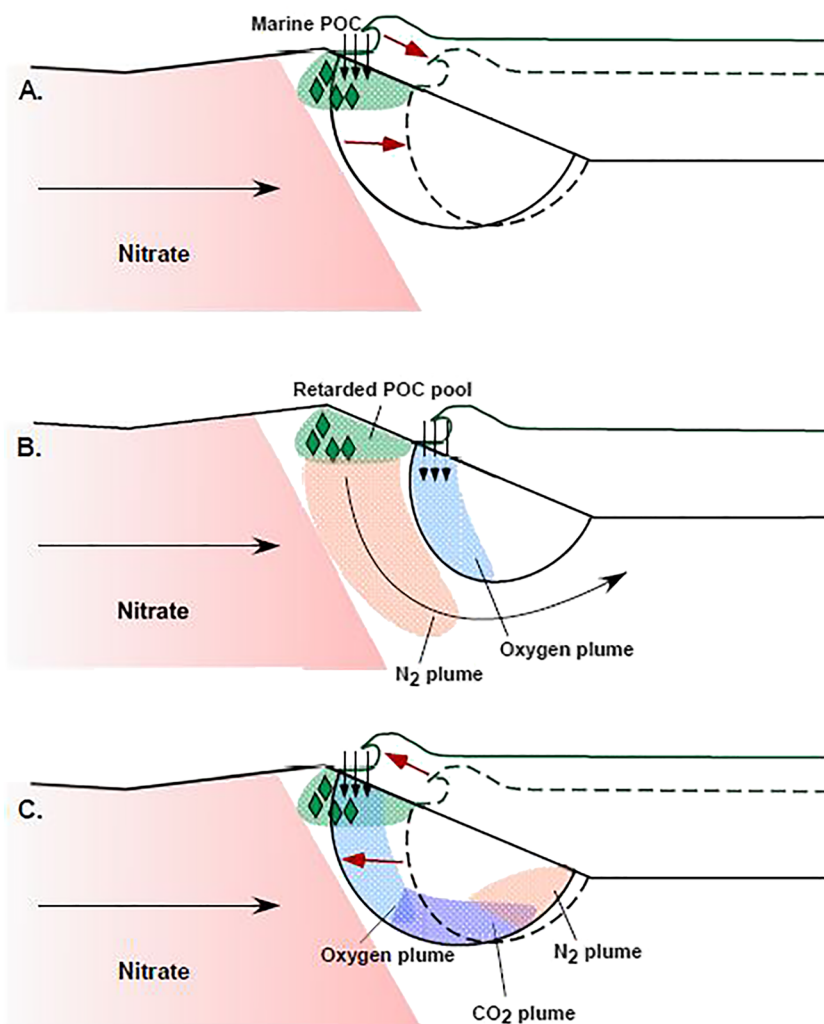


Figure 1. Conceptual model of particulate organic carbon contributions to biogeochemical reactions within the intertidal zone of beach aquifers based on results of Kim et al. (2019). (a) Marine POC is delivered to the aquifer through seawater infiltration during wave and tide activity (solid lines). Hydrologic transience moves the salinity distribution (red arrows to dotted lines), but the pool of POC is retarded relative to groundwater advection. (b) Retarded POC supports reactions, such as denitrification, outside of circulating saline groundwater flow paths. (c) As hydrologic conditions change, the circulation cell shifts landward to encompass the pool of POC. This heightens denitrification toward the end of the flow path where conditions tend to be anoxic. The hot spot of N₂ gas production shifts seaward of the circulation cell.

biogeochemical redox reactions may occur over these carbon pools, contributing to the spatial heterogeneity of reaction zones and overall reactivity of beach aquifers (Kim et al., 2019). Further, overall reactivity of beach aquifers may have an “ebb and flow,” congruous with a transient hydrologic framework moving across a heterogeneous patchwork of POC pools.

In this work, we show that the retarded movement and resulting heterogeneous distribution of POC, traditionally disregarded in beach biogeochemical reactions, can contribute to reaction intensity and the distribution of reaction zones within beach aquifers. Groundwater flow and reactive transport models were used to understand how POC, retarded compared to groundwater advection, alters the biogeochemical efficiency of beach aquifer systems due to hydrologic transience. Results demonstrate the transient contributions of POC to redox reactions within aquifer systems and show that POC deposition location and hydrology affect the reactivity of intertidal sediments. This suggests that the reactive potential of beach sediments is greater than previously conceptualized.

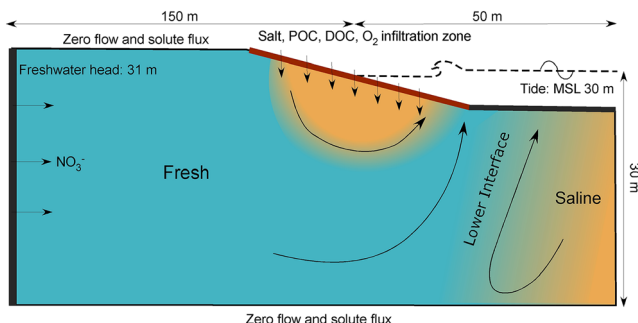


Figure 2. Numerical model schematic.

2. Numerical Simulations

Modeling was conducted in two stages. Variable-density groundwater flow, salt transport, and POC transport with retardation were first simulated using SEAWAT v4.0 (Langevin & Guo, 2006; Langevin et al., 2007; section 2.1). The distribution of POC and the groundwater flow field obtained from SEAWAT was then coupled to a reactive transport model using PHT3D v2.13 (Prommer & Post, 2002) to simulate aerobic respiration and denitrification in tidally influenced beach aquifers (section 2.2).

2.1. Phase I: POC Transport Model

Groundwater flow and salt transport were simulated for a homogeneous and unconfined coastal aquifer, with seaward freshwater discharge and intertidal circulation of seawater. From the beachface-mean sea level (MSL) intersection, the domain extended 150 m landward, 50 m seaward, and 30 m vertically. The grid had 125 layers and 184 columns, with higher discretization ($dx = 0.31$ m, $dy = 0.06$ m) in the intertidal zone (following Robinson et al., 2007 and Heiss et al., 2017).

The landward vertical boundary was set as a constant-head Dirichlet boundary with a constant salinity of 0 ppt (Figure 2). The periodic boundary condition (PBC) package (Post, 2011) was used to apply multiple sinusoidal tidal fluctuations along the right boundary, with time-varying head calculated as follows:

$$h_t = h_0 + A \cos(xt - \varphi) \quad (1)$$

where h_t (m rel. MSL) is the tide elevation at time t , h_0 (m) is MSL, A (m) is tidal amplitude, x (rad day $^{-1}$) is the tidal angular frequency, and φ (rad) is the phase shift. Five tidal constituents were used in the model, effectively simulating the movement of the intertidal circulation cell over spring-neap timescales based on field observations at Cape Shores, Lewes, DE (Heiss et al., 2017; supporting information Table S1). This allowed the POC pool, static within the beach aquifer, to be utilized as a carbon source for microbial respiration at different times in response to the movement of the circulation cell. Infiltrating seawater along the aquifer-ocean boundary was assigned a salinity of 35 ppt, while a zero-concentration gradient was set for outward flow. Zero flow and solute flux were assigned to the bottom, the seaward vertical boundary, and the top of the model domain landward of the shoreface.

A linear isotherm was assumed for sorption and a retardation factor was used to simulate the transport of POC. The retardation factor was calculated using the equation:

$$R = 1 + \frac{\rho_b}{\theta} K_d \quad (2)$$

where R is the retardation factor, ρ_b is the bulk density in g/cm 3 , θ is porosity, and K_d is the distribution coefficient. R for the base case was calculated using ρ_b , θ , and K_d values based on Cape Shores, Lewes, DE, to yield a retardation factor of 1.416 (Davis, 2000; Krupka et al., 1999); see supporting information (Table S2 and Text S1). A range of K_d [R] values were tested in the sensitivity analysis.

In environmental settings, the cross-sectional distribution of POC within the aquifer at a given time reflects transient processes of continuous infiltration, degradation, and transport (Kim et al., 2019). After multiple diurnal cycles of seawater infiltration and POC degradation, the in situ distribution of POC will be heterogeneous and unrelated to the salinity distribution due to hydrologic shifts. Despite eventual advection throughout the aquifer, carbon, bacteria, and particulate material from infiltrating seawater can become entrained in beach sands (Couturier et al., 2016; Gast et al., 2015). To represent this process, a constant influx ($C = 1$, unitless and later normalized to a concentration) of a solute representing POC was assigned along the shoreface boundary. Infiltration was set to only occur between the high tide line and the midtide line with seawater infiltration. This was done to represent the influx of POC from accumulation of beach wrack that predominantly occurs from middle- to high-tide mark, rather than linearly across the entire seawater infiltration zone (low- to high-tide mark) (Orr et al., 2005; supporting information Figure S1). Due to retardation and transient saltwater infiltration from spring-neap cycling, POC never reached a steady state distribution.

Table 1

Reaction Network and Kinetic Rate Expressions (adopted from Bardini et al. [2012] and Heiss et al. [2017])

| Name | Reaction | Rate expression |
|---------------------|--|---|
| DOC Degradation | $\text{DOC} \rightarrow \text{CO}_2$ | Rate = $k_{\text{fox}}[\text{DOC}]$; |
| Aerobic Respiration | $\text{OC} + \text{O}_2 \rightarrow \text{CO}_2 + \text{H}_2\text{O}$ | If $[\text{O}_2] > \text{kmo2}$; Rate = $k_{\text{fox}}[\text{DOC}] + k_{\text{fox}}[\text{POC}]$; If $[\text{O}_2] < \text{kmo2}$; Rate = $(k_{\text{fox}}[\text{DOC}] + k_{\text{fox}}[\text{POC}]) \times ([\text{O}_2]/\text{kmo2})$ |
| Denitrification | $5\text{OC} + 4\text{NO}_3^- + 4\text{H}^+ \rightarrow 5\text{CO}_2 + 2\text{N}_2 + 7\text{H}_2\text{O}$ | If $[\text{O}_2] > \text{kmo2}$; Rate = 0; If $[\text{O}_2] < \text{kmo2}$ and $[\text{NO}_3^-] > \text{kmo3}$; Rate = $(k_{\text{fox}}[\text{DOC}] + k_{\text{fox}}[\text{POC}]) \times (1 - [\text{O}_2]/\text{kmo2})$; If $[\text{O}_2] < \text{kmo2}$ and $[\text{NO}_3^-] < \text{kmo3}$; Rate = $(k_{\text{fox}}[\text{DOC}] + k_{\text{fox}}[\text{POC}]) \times (1 - [\text{O}_2]/\text{kmo2}) \times ([\text{NO}_3^-]/\text{kmo3})$ |

Note. OC indicates Organic Carbon and can represent both POC and DOC. k_{fox} is the rate constant for the decomposition of OC, kmo2 the limiting concentration of O_2 , and kmo3 the limiting concentration of NO_3^- .

Therefore, once the salinity distribution reached dynamic steady state, the average of the POC distributions over three spring-neap cycles was taken to be representative of POC distribution within the aquifer. The distribution was then scaled in its concentration such that the total amount of POC in the circulation cell was 10 mg. This ensured that all model cases, despite differences in POC geometry and spatial extent, had the same total amount of POC introduced within the aquifer (except for cases with varying POC concentrations). Further, utilizing five tidal constituents created differences in tidal amplitude between every spring tide within the model. Therefore, rather than picking one representative spring or neap tide POC distribution, we integrated over three spring-neap cycles to obtain a time-averaged POC distribution. The retardation factor and the tidal amplitude were varied during Phase I to obtain a set of POC distributions. Each POC distribution was assigned as a constant concentration within the aquifer for Phase II reactive transport modeling, in which reactions and additional reactive solutes (DOC, O_2 , CO_2 , NO_3^- , and N_2) were introduced.

2.2. Phase II: Reactive Transport Model

DOC degradation, aerobic respiration, and nitrate removal via denitrification were simulated as kinetic multi-species reactions to investigate the contribution of POC to beach reactivity. Constant concentrations of O_2 (313 μM) and DOC (60 μM) were assigned across the shoreface, and NO_3^- (129 μM) was assigned to fresh groundwater inflow along the landward vertical boundary. O_2 and DOC had an initial concentration of zero within the aquifer, and CO_2 and N_2 were assigned as mobile kinetic species produced as a byproduct of aerobic respiration and denitrification, respectively. DOC was only introduced to the aquifer when the carbon reaction rate, and DOC and POC concentrations were varied to assess the relative importance of POC concentrations (section 3.5). The initial NO_3^- concentration was assigned according to salinity; fresh pore water was assigned the maximum nitrate concentration (129 μM), and fully saline pore water was assigned a concentration of zero. POC was assigned as an immobile kinetic species within the aquifer, with its location and geometry prescribed from Phase I. No advection or degradation was assigned to POC for Phase II simulations to ensure a steady state distribution. Concentrations used for O_2 and NO_3^- were based on previous literature (Heiss et al., 2017), while the range of POC and DOC values tested were obtained from field measurements at Cape Shores, Lewes, DE (Kim et al., 2019). The reaction network and the kinetic rate expressions (Table 1) were adapted from previous work (Bardini et al., 2012; Heiss et al., 2017; Kim et al., 2017).

2.3. Sensitivity Analysis

A base case model was developed after Heiss et al. (2017) using the parameters listed in Table 2. Various physical and chemical parameters in Phases I and II were varied to identify the factors that control reactivity that is fueled by POC. Only one variable either from Phase I or Phase II was altered for a given model case. Variations to Phase I variables (K_d or tidal amplitude) while obtaining a POC distribution were always run with base case values for Phase II variables. Similarly, changes to Phase II variables that controlled the movement of dissolved solutes were always run with a POC distribution that was obtained using Phase I base case values of deposition. To isolate contact-induced reactivity, parameters were not covaried in both Phases I and II.

Table 2

Parameter Values Used for the Base Case Model and Range of Parameter Values Used for Sensitivity Analyses

| Parameter | Sensitivity values | Base case value |
|---|---|-------------------------------------|
| <i>Phase I—POC Deposition</i> | | |
| $K_d [R]$ | 0.1, 0.5 1, 2, 10 [1.416, 3.08, 5.16, 9.33, 51.6] | 0.1 [1.416] |
| Tidal Amplitude | 0.3, 0.5, 0.6, 0.7, 0.9 m | 0.6 m |
| <i>Phase II—Reactive Transport of Dissolved Solutes</i> | | |
| Hydraulic Conductivity | 0.5, 3, 6, 9, and 12 m/day | 3 m/day |
| Tidal Amplitude | 0.3, 0.5, 0.6, 0.7, and 0.9 m | 0.6 m |
| Total POC Mass | 83, 249, 832, 1,248, and 2,081 μmol (1, 3, 10, 15, and 25 mg) | 832 μmol |
| DOC Concentration | 5, 10, 30, 60, and 120 μM | 60 μM |
| Carbon Reactivity ($k_{\text{fox}}^{\text{a}}$) | 1.5×10^{-7} , 4.0×10^{-7} , 1.5×10^{-6} , 4.0×10^{-6} , and $1.5 \times 10^{-5} \text{ s}^{-1}$ | $1.5 \times 10^{-6} \text{ s}^{-1}$ |
| <i>Phase II Unvaried</i> | | |
| $k_{\text{mo2}}^{\text{a,b}}$ | - | $3.125 \times 10^{-5} \text{ M}$ |
| $k_{\text{mn03}}^{\text{a,b}}$ | - | $8.065 \times 10^{-6} \text{ M}$ |

Note. Phase I parameters relate to conditions during POC deposition while Phase II parameters relate to reactive transport modeling after a POC distribution has been determined.

^aWang and Van Cappellen (1996). ^bBardini et al. (2012).

Phase I variables (retardation factor and tidal amplitude of POC deposition) were varied to test the importance of the spatial distribution of POC. For each parameter varied, four different POC distributions were generated. All cases had a total POC mass of 10 mg. POC area was calculated by summing up the model cell areas that had POC concentrations greater than 0.01 μM . Hydrologic conditions during the Phase II reactive transport simulation were held constant at base case conditions, and thus, the set of simulations demonstrates the effect of antecedent hydrologic conditions on beach reactivity.

Phase II variables controlled the reactivity of the system by varying carbon concentrations and the mobility of other dissolved reactants (O_2 , NO_3^- , and DOC). Base case POC was deposited using base case values of hydraulic conductivity and tidal amplitude in Phase I. Simulations with the base case POC distribution were then run with varying hydraulic conductivity and tidal amplitudes (Phase II variables) to understand how hydrologic properties that affect the movement of reactants, following a POC deposition event, relate to POC utilization. While changes to hydraulic conductivity between POC deposition and reactant mobilization are unrealistic, these model cases showcase the effects of differential distribution between POC and mobile, dissolved reactants. To understand how nitrogen removal depends on chemical conditions, total POC mass, infiltrating DOC concentration, and carbon reactivity were varied while holding other parameters at base case values.

The mass of nitrate removed from the system was quantified over time by integrating the denitrification rate of each model grid cell in the beach aquifer. We also calculated the “Exposure Area,” defined as the percent area of the circulation cell where conditions for denitrification were favorable. Areas favorable for denitrification were located where pore water was >50% freshwater (50% salinity), oxygen concentrations were lower than the threshold value (<31.2 μM), and POC concentrations were >0.01 μM .

The dimensionless Damköhler (Da) number was calculated to assess the relative balance between advection and reaction time scales across model cases (e.g., Briggs et al., 2015; Gu et al., 2007; Heiss et al., 2017; Ocampo et al., 2006; Zarnetske et al., 2012). Da is defined as follows:

$$\text{Da} = k_{\text{fox}} \times \frac{v_s}{Q}$$

where k_{fox} is carbon reactivity [T^{-1}] and $\frac{v_s}{Q}$ the residence time of saltwater within the saline circulation cell [T]. The residence time was calculated by dividing v_s [L^3], the volume of saltwater in the saline circulation cell, by the influx of saltwater per unit length of shoreline [L^3/T]. A Damköhler number of 1 indicates that the reaction rate is balanced by the advective delivery of mobile reactants. With higher reaction rates or lower advective rates, $\text{Da} > 1$ and the reactivity of the system is limited by the delivery of reactants. Conversely, $\text{Da} < 1$ implies that the system is reaction rate limited (i.e., solute supply outpaces microbial demand).

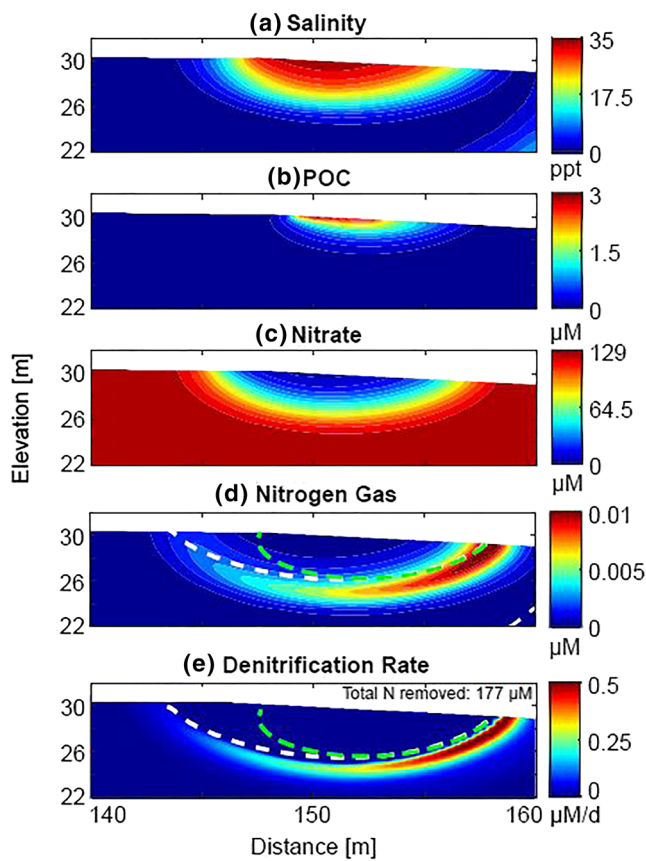


Figure 3. Solute distributions for a base case scenario (a) salinity, (b) POC, (c) nitrate, and (d) nitrogen gas. (e) Denitrification rates from a selected day between spring-neap tide are shown. Dotted line (d: black and e: green) indicates the location of POC ($0.01 \mu\text{M}$), while the white solid line in indicates 50% seawater. A total of $177 \mu\text{M}$ of nitrate was removed for the day shown.

3. Results

3.1. POC and Reactivity Distribution—Base Case

Tidal infiltration of seawater across the beachface created an intertidal circulation cell, consistent with previous field and modeling studies of the intertidal zone (Heiss & Michael, 2014; Kim et al., 2017; Michael et al., 2005; Robinson et al., 2007). Retardation of POC relative to advection created a pool of POC in the shallow beach beneath the infiltration zone. Figure 3 shows conditions from a base case scenario for a day arbitrarily selected between spring-neap tide, Day 113.

Nitrate removal via denitrification occurred along the freshwater-seawater mixing zone as nitrate-rich freshwater came into contact with POC (Figure 3), producing N_2 gas (Figure 3d), which was transported along the groundwater flow path to the discharge zone. This is consistent with previous field and modeling findings (e.g., Heiss & Michael, 2014; Kim et al., 2017, 2019). The N_2 plume was proximal to the boundary of the POC pool and centered in the mixing zone (Figure 3d, white dotted line), due to the necessary contact between POC and nitrate-rich water for POC-supported denitrification. This is supported by the spatial distribution of denitrification rate (Figure 3e).

3.2. Temporal Variations in POC-Supported Denitrification

Spring-neap changes in the geometry of the circulation cell resulted in temporal variability of POC utilization (Figure 4). The pool of POC intermittently fueled denitrification, contingent on the spatial overlap between POC and low-oxygen, NO_3^- -rich water. Figure 4 displays the transient nature of POC-supported denitrification. With changing tidal stage, the zone of saline water infiltration moved laterally seaward and landward on the beachface. Higher tidal amplitudes during spring tide expanded the extent of the circulation cell. This allowed oxic seawater infiltration where POC was located, effectively limiting its use for denitrification. As tidal amplitudes fell, the circulation cell contracted, which increased overlap between POC and anoxic water, allowing POC to be utilized for denitrification when NO_3^- was present. Although the exposure area was

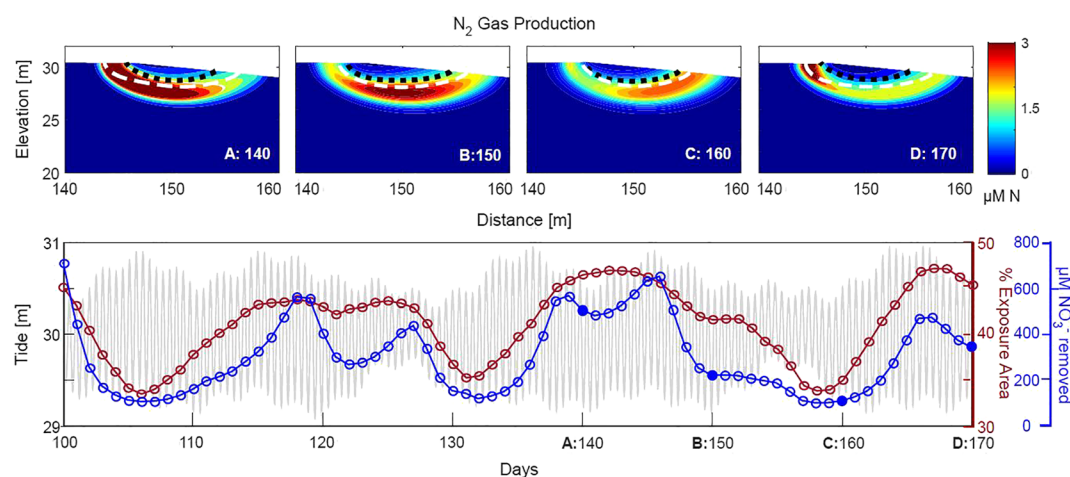


Figure 4. Simulated temporal variations in POC-supported denitrification for the base case scenario. (upper panel) Spatial distribution of nitrogen gas hot spots as hypothesized in Figure 1. White dotted line indicates 50% salinity, black dotted line outlines POC location, and white text indicates model day shown. (lower panel) Tidal signal (gray), total NO_3^- removed (blue), and % exposure area (red) over time. The two curves covary over spring-neap cycles.

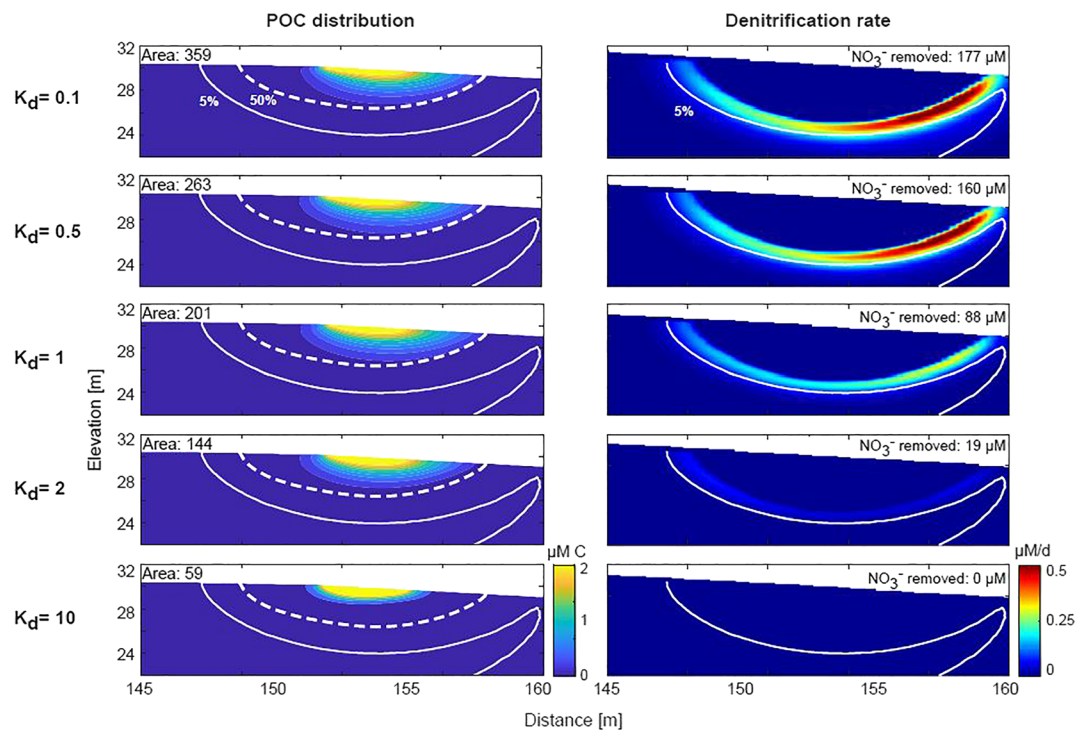


Figure 5. Distributions of POC with different K_d values during Phase I POC deposition and resulting denitrification rate following base-case Phase II simulation. Total NO_3^- removal for Day 113 is also indicated. The total mass of POC is constant across model cases. Lower K_d resulted in a more elongated and vertically expansive POC zone, with area of POC (model cell area above 0.01 μM) increasing with lower K_d . With a larger zone of POC, total NO_3^- removal also increased.

conservatively defined as more than 50% freshwater, it is expected that denitrification will occur at lower salinities. As salinity is just an indicator where denitrification is likely to happen, this accounts for the deviation between exposure area (Figure 4, lower panel red) and total NO_3^- removed (Figure 4, lower panel blue) over time. Further, Figure 4 shows that there is a slight time lag (~5 days) between tidal amplitude conditions and salinity response within the intertidal zone. This subsequently leads to a lag between tidal amplitude and reaction response, indicating asynchronous tidal and chemical conditions within beach systems. Overall, the simulation shows that hot spots of denitrification migrate within the beach, supported by in situ POC. In natural settings, where POC distributions are dynamic with changes in tidal amplitude, more denitrification may occur as a result of increased tidal amplitude, subsequent increases in POC infiltration, and greater contact between nitrate and POC.

3.3. Impacts of POC Spatial Distributions on Nitrate Removal

The effect of the spatial distribution of POC (or antecedent hydrologic conditions) on denitrification was explored by varying the retardation factor (i.e., K_d) and the tidal amplitude during POC deposition. All cases were scaled to have the same mass of total POC within the aquifer.

The changing spatial distribution of POC from varying retardation altered NO_3^- removal rates. With a lower K_d value, the pool of POC developed an elongated tail seaward and had a larger area (Figure 5). With increasing K_d , the POC distribution decreased in both its vertical and horizontal extent. With a larger K_d , the POC was located in the shallow beach subsurface in the interior of the saltwater circulation cell and not in contact with anoxic nitrate-rich groundwater. This reduced the magnitude and areal extent of denitrification. Compared with the base-case scenario ($K_d = 0.1$) that removed 177 μM of NO_3^- , cases with K_d values of 0.5, 1, 2, and 10 removed 160 μM , 88 μM , 19 μM , and 0 μM , respectively. This indicates that a large, dispersed POC pool is more effective at fueling denitrification than a concentrated, smaller POC pool with the same total carbon mass due to an increase in contact with nitrate. POC has been found in beach aquifers in

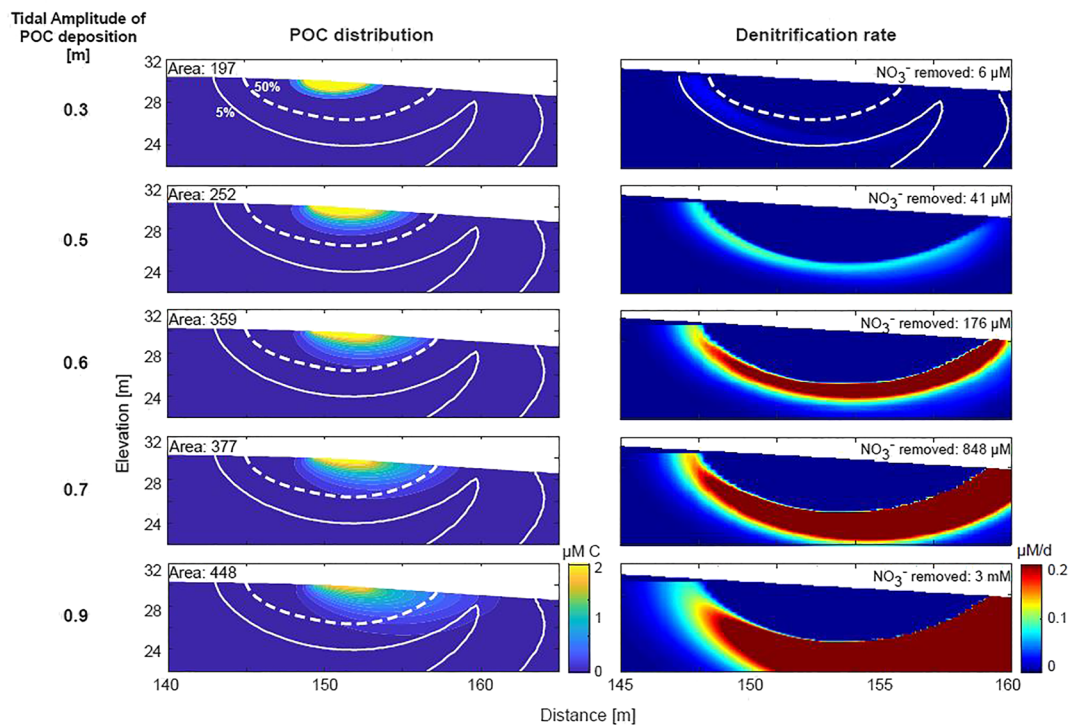


Figure 6. POC distribution for different tidal amplitudes during Phase I POC deposition (left panels) and resulting denitrification rate following base-case Phase II simulation (right panels). Total POC mass for all cases was held constant (10 mg). With increasing tidal amplitudes, the POC extent was larger. POC area is indicated (left panels). Denitrification rates for Day 113 are shown (right panels), with total NO_3^- removal (text within panels) quantified for that day by integrating the denitrification rate of each model grid cell across the full model domain. Nitrate removal increases with an increase in the areal extent of POC.

both well-defined and elongate pools (e.g., Kim et al., 2017, 2019), which suggests that retardation may vary along transport paths, though only a single retardation factor was considered in this study.

The areal extent of POC greatly expanded with an increase in tidal amplitude (Figure 6). As was the case with larger POC pools for lower K_d values, the larger pool of POC associated with larger tidal amplitudes increased nitrate removal despite containing the same amount of carbon. For example, the model case with a 0.9 m tidal amplitude removed 3,000 μM NO_3^- while the case with 0.3 m tide removed 6 μM . Therefore, large areas of POC that result from previous high tidal conditions (spring tide) and storm surge may increase the magnitude and area of nitrate removal within the beach aquifer.

3.4. Influence of Hydraulic Conductivity and Tidal Amplitude on POC Utilization

Hydraulic conductivity affected total denitrification in the beach by altering the areal extent of the saline circulation cell and groundwater flow rates. Higher hydraulic conductivity resulted in greater freshwater flux, which decreased the extent of the circulation (Heiss & Michael, 2014; Kuan et al., 2012) (Figure 7). Smaller circulation cells associated with higher K values allowed greater contact between NO_3^- and POC, which increased overall NO_3^- removal as hydraulic conductivity increased.

Higher K also increased the difference in the size of the circulation cell between spring and neap tide, thereby increasing the range of in the NO_3^- removal between spring and neap tide (Figure 7, bottom panel). This illustrates the complex relationship between aquifer properties and the spatial overlap of reactants for optimal POC utilization.

Increasing tidal amplitude similarly impacted total denitrification by altering the spatial overlap between POC and dissolved reactants. With increasing tidal amplitude, the extent of the saline circulation cell increased, and POC exposure area decreased by allowing oxic water to overlap with POC (Figure 8, top

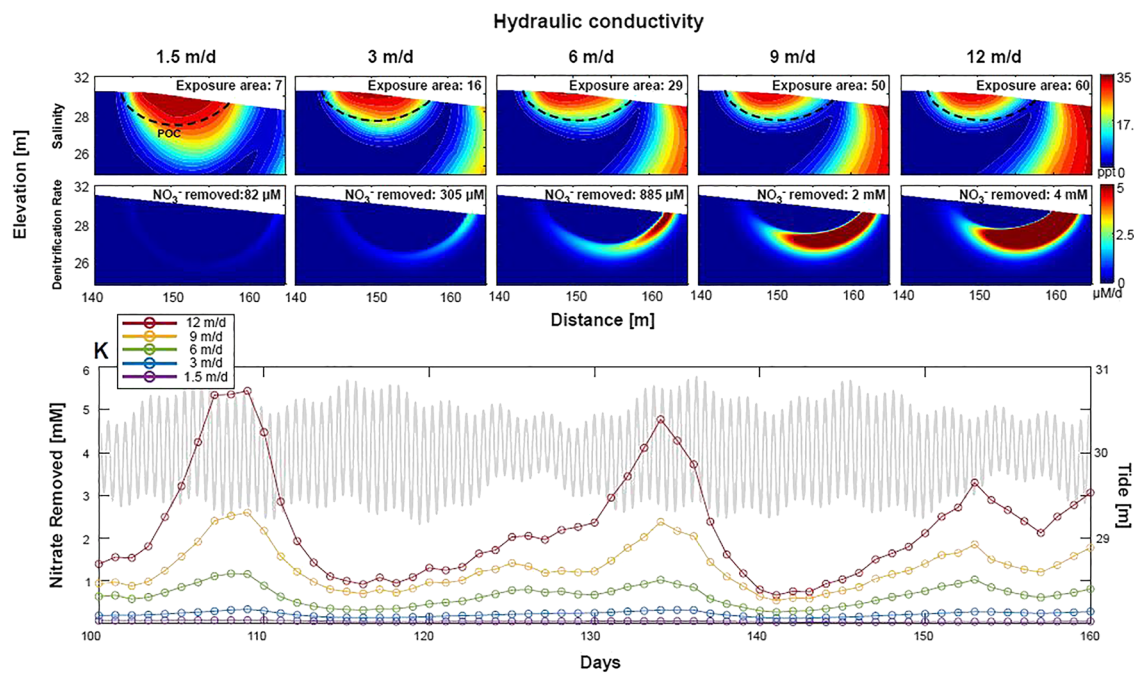


Figure 7. Effects of increasing hydraulic conductivity in Phase II on POC utilization in beach aquifers using base-case Phase I POC deposition scenario. (top row) Higher K allows for increased freshwater flux, decreasing the areal extent of the circulation cell and allowing inland encroachment of the lower interface. Extent of POC (black dotted line) and exposure area is indicated within the panel. (middle row) Denitrification rates (colors) and nitrate removed (text) for Day 113 for each model scenario. Smaller circulation cells resulting from higher K allow for more contact between anoxic water and POC, increasing denitrification. (bottom panel) Effects of K on NO₃⁻ removed over time.

This hindered POC utilization for nitrate removal and decreased denitrification (Figure 8, middle row). POC was deposited using a tidal amplitude of 0.6 m. When the tidal amplitude for the infiltration of reactive

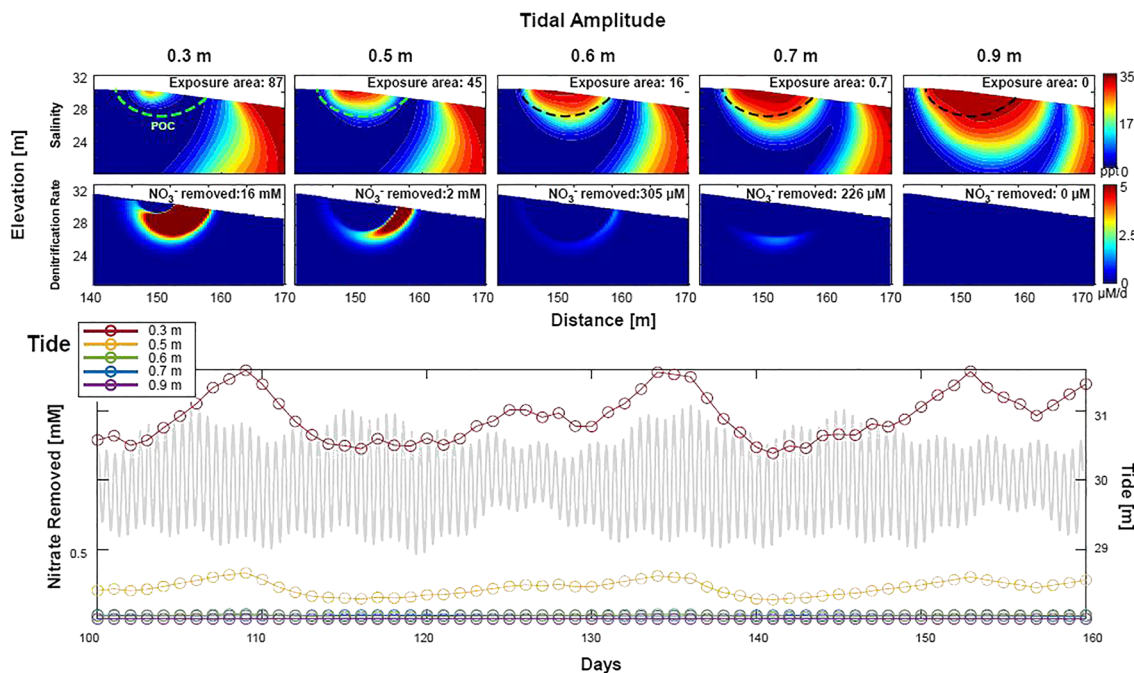


Figure 8. Effects of tidal amplitude in Phase II (TA = 0.3, 0.5, 0.6, 0.7, and 0.9 m) on nitrate removal within the intertidal zone using the base-case Phase I POC deposition scenario. (top row) Changing salinity distributions with increasing tidal amplitude. POC is indicated in green or black dotted line. POC exposure area is indicated in text. (middle row) Denitrification rates (colors) for Day 113 with total NO₃⁻ removed (text). (bottom panel) Nitrate removal over time.

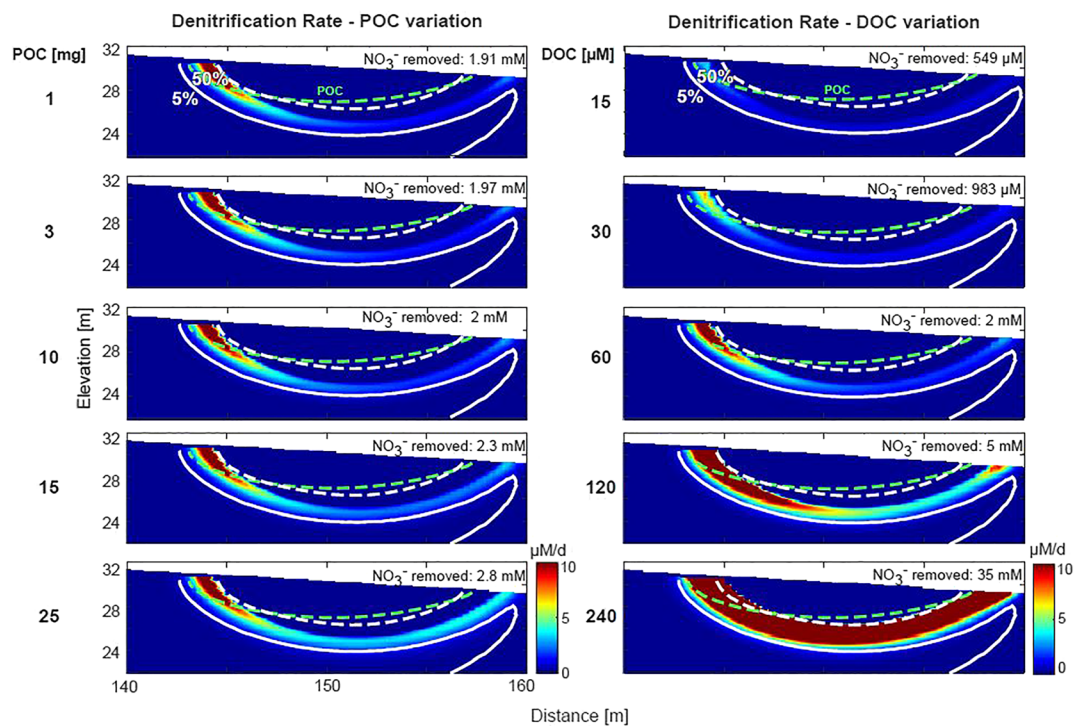


Figure 9. Effects of POC and DOC concentrations on nitrate removal on Day 113. Colors indicate denitrification rates. (left column) POC concentrations were varied while DOC concentrations were held at base case values. Green dotted line indicates the location of POC, white dotted line 50% salinity and solid white line 5% salinity. (right column) DOC concentrations were varied while POC concentrations were held at base case values. The total mass of nitrate removed for Day 113 is indicated on each panel.

solutes in became greater than the 0.6 m amplitude used during initial POC deposition, POC was completely engulfed by the saline circulation cell and little to no POC was exposed to high- NO_3^- , low- O_2 groundwater. This indicates that POC utilization is increased when a smaller-tidal amplitude event is followed by a larger tidal amplitude of POC deposition, provided that the POC does not degrade too quickly and remains within the beach.

3.5. Carbon Characteristics and Impacts on Nitrate Removal

To understand the effects of carbon concentrations and carbon reactivity on denitrification, both POC and DOC were introduced as carbon sources. Both POC (within the model) and DOC (influx) concentrations were varied and cases were compared to understand changes in the spatial patterns of denitrification (Figure 9). Regardless of carbon form, increasing the amount of total carbon (POC + DOC) increased denitrification within the intertidal zone. However, there were spatial differences in denitrification activity, depending on the source of carbon. Spatial patterns of denitrification rates did not change substantially with higher concentrations of POC, because the spatial overlap between POC and NO_3^- is a necessity for POC-supported denitrification, and the system was not carbon limited. (POC does not degrade within the model.) On the other hand, reaction rate patterns were altered significantly with increasing DOC concentration, with the areal extent of elevated reaction rates increasing along the freshwater-seawater mixing zone as DOC concentration increased. This was due to faster depletion of O_2 along seawater flow paths, which allowed anoxic conditions to occur earlier along flow paths. This shows that while POC-supported denitrification is spatially constrained to the distribution of POC, DOC-supported denitrification, contingent on DOC concentration and subsequent oxygen drawdown, is spatially variable.

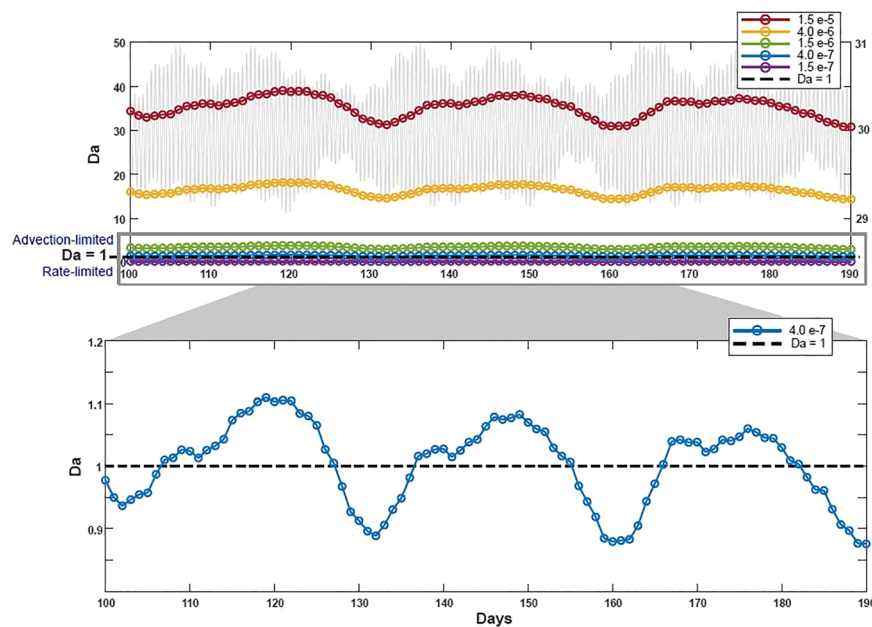


Figure 10. Damköhler (Da) number over time for base case parameters using a range of carbon reactivity values with tidal signal shown in gray. Da values fluctuate with the changing saltwater volume in the circulation cell over time. For the model case with reactivity of $4.0 \times 10^{-7} \text{ s}^{-1}$ (blue), Da varies between advection limited ($\text{Da} > 1$) and rate limited ($\text{Da} < 1$) as the size of the circulation cell, and the residence time, changes.

Altering DOC reactivity modified the relative balance between advective DOC supply and denitrification. In all models, the Damköhler number fluctuated over spring-neap cycles due to expansion and contraction of the circulation cell and associated changes to the residence time of circulating groundwater (Figure 10). Low DOC reactivity resulted in Damköhler numbers < 1 , forcing the system to rate limited. Conversely, higher DOC rate constants led to higher reactivity rates and increased Da, forcing the system to become advection-limited. With higher reaction rates, the quantity of nitrate removed also increased.

At certain reaction rates, the Damköhler number fluctuated between advection limited ($\text{Da} > 1$) and rate limited ($\text{Da} < 1$) as the extent of the saline circulation cell changed over spring-neap cycles (Figure 10, lower panel). These results demonstrate for the first time the transient behavior of in beach biogeochemical reactions and the intermittent use of POC as an electron donor. With changing hydrologic conditions, the relative importance of POC may be increased when systems are DOC supply limited ($\text{Da} > 1$) due to lower advection. Overall, results show that higher POC and DOC concentrations and higher carbon reaction rates increase denitrification within the intertidal zone.

4. Discussion

The results of this study highlight the importance of the spatial relationship between POC and mobile solutes (O_2 , NO_3^-) in POC-supported denitrification. Because contact between POC and anoxic, NO_3^- -rich water was a necessity for denitrification, physical factors that allowed for different spatial distributions of POC and O_2 increased nitrate removal. This was achieved with more expansive POC pools, either from a lower K_d or a larger depositional tidal amplitude. Similar results were achieved when there was a large difference between POC-depositional conditions and succeeding hydrologic conditions, resulting from differences in hydraulic conductivity and tidal amplitude (post-POC deposition). Reactions were supported as hydrologic conditions responsible for POC deposition shifted to expose POC to NO_3^- -rich water, resulting in a “carbon memory” effect. Because this spatial relationship between POC and other solutes were contingent upon hydrologic conditions, there were variations in the utilization of POC with hydrologic transience (Figures 4 and 10). As the extent of the saline circulation cell changed over spring-neap cycles, the areal extent of POC and NO_3^- contact also fluctuated, impacting total nitrate removed on a given day. This emphasizes the temporally variable contribution of POC to beach reactions. Further, while sensitivity

analyses of various model parameters (K_d , tidal amplitude, and hydraulic conductivity) were only conducted with POC as the sole carbon source, it is highly likely that surface water with POC would often have an associated DOC fraction. Therefore, the relative contributions of POC to reactions, in addition to its absolute contributions, would likewise be transient contingent upon its relationship with DOC. In environments with low DOC influx or high DOC reactivity, the importance of POC as an alternative carbon source, given its spatial accessibility, would increase.

In the model setup considered, POC was specified as a constant concentration and did not degrade with time to ensure that POC concentrations were static over the duration of the simulations. This reduced the importance of its concentration and drove models to be rate limited. However, when carbon reaction rates were varied, systems with faster reaction rates became advection limited (Figure 10). This shows that in addition to the spatial relationship between POC and solutes, the balance between reaction rate and POC amount would also affect POC utilization and its persistence over time. In systems with highly refractory POC, an expansive pool of POC may not be as biogeochemically utilized despite its large spatial extent and accessibility. In contrast, a small but highly labile pool of POC located in a favorable geometric position with other solutes may support a more impactful hot spot or hot moment of chemical reactions.

While temporal changes to reaction characteristics were only induced by hydrologic transience in this study, distributions of POC are not static in field settings. Therefore, interactions between POC and the beach system are expected to occur over various timescales. On spring-neap timescales, as explored in this study, results highlight that antecedent hydrologic conditions are as pertinent to beach reactivity as much as the current conditions. For example, an expansive POC pool from a large spring tide combined with a decreasing tidal amplitude would increase biogeochemical activity relative to a rising tide system that deposited POC during neap tide. On finer timescales (waves, diurnal tides) with smaller changes to the spatial geometry of the circulation cell, POC degradation rate and reactant delivery at a certain location may be more relevant than the spatial accessibility of POC as a carbon source. While we expect the most drastic changes to POC geometry (due to its degradation and transport) to occur over spring-neap cycles based on field results (Kim et al., 2019), highly reactive pools of POC have the potential to create hot spots and hot moments of biogeochemical reactions on shorter timescales. In addition, while most marine POC is expected to readily react and not persist over seasonal timescales (Seidel et al., 2015), there are seasonal changes to primary production that would alter the infiltration concentrations of POC and DOC into beach aquifers. This suggests that the total amount of POC within the aquifer would covary, to some extent, with seasonal primary production, altering the magnitude of POC-supported reactions.

While various parameters were adjusted to identify conditions that allow for increased utilization of POC in beach reactivity, more complex dynamics of POC utilization are expected in field settings. The models in this study were designed so that some spatial overlap between POC and ideal reaction conditions would exist. The POC distribution is highly simplified within this model. However, the geometric relationship between POC and the circulation cell is expected to be more dynamic in field settings. Topography, geologic heterogeneity, grain size, continuous advection, and differential POC fragmentation/degradation are all expected to disperse POC in more complex patterns than idealized in this study (Kim et al., 2019). This implies that reactivity supported and maintained by POC within the beach would be spatiotemporally patchier, further deviating from expected locations according to oxygen concentrations along groundwater flow paths. Geologic heterogeneity, anisotropy, and dispersion, while not varied in this study, would likely influence transport paths and the distribution of POC (Gelhar et al., 1992; Heiss et al., 2020; Rocha et al., 2005; Sawyer, 2015). While the medium used within the model is homogeneous and isotropic, heterogeneity would likely affect POC filtration due to differential filtering in different sediments. As POC infiltrates, adsorption may change permeability and K_d along the infiltration flow path. Changes in K over time due to differential POC filtration may produce POC distributions within the aquifer that are heterogeneous, affecting the formation of biogeochemical “hot spots” and “hot moments,” in turn affecting POC oxidation. While the simplified models in this study did not explicitly consider these geological-hydrological-biogeochemical feedbacks, the model setup was able to capture the importance of contact between POC and reactive species on biogeochemical processing in the beach. Additionally, changes to permeability and porosity due to POC filtration are likely to be minimal due to the small particulate sizes that are readily advected with groundwater flow.

This study explored the impacts of immobile POC pools on beach reactivity and, in doing so, made various assumptions of the chemical behavior of POC. Considering more realistic representation of POC behavior in models would increase the transience and complexity of POC contributions to beach biogeochemistry than simulated in this study. To ensure a steady-state distribution of POC, no POC degradation was considered in the model cases presented. However, in natural systems, degradation of POC in beach sediments may alter the concentration, spatial extent, and transport paths over time, and geologic and chemical heterogeneity will also likely affect chemical speciation in the intertidal zone. In addition, while this study employed a single DOC rate constant, DOC reactivity is likely to change along transport paths (Seidel et al., 2015). Competition between POC and DOC as an electron donor would likely influence the supply and distribution of both carbon pools. As POC degrades, leaching of DOC from POC is expected (Kim et al., 2019), which would also influence DOC availability within the aquifer. As the form of carbon supplied to the beach aquifer can be highly diverse (invertebrates, macrophytes, seagrass, woody debris, and offshore oil spills), further work is required to better resolve the relationship between POC reactivity and biogeochemical reactivity in beach aquifers.

Lastly, the contributions of POC to beach biogeochemistry were only quantified using denitrification. However, POC within beach sediments can support other redox reactions that require a carbon source. While POC-mediated denitrification decreased with increasing overlap with oxic, saline water, reactions that require seawater-derived reactants, such as sulfate reduction, may conversely be enhanced (Heiss et al., 2017). Depending upon solute distributions, a POC pool may simultaneously support denitrification, iron transformation, and sulfate reduction (McAllister et al., 2015). Field and modeling investigations of POC pools also show that POC not only supports chemical reactions but is also a source of DOC and other nutrients (particulate nitrogen, ammonium, phosphate, and particulate phosphorus) via degradation and leaching (Heiss, 2020; Kim et al., 2019). Though our models assumed that no additional nutrients were released from the pool of POC, POC may be a source rather than a sink of nitrogen through ammonification in natural settings. Thus, POC pools may serve as a repository of nutrients in settings with abundant organic matter (i.e., Kim et al., 2019). Therefore, while this study focused on identifying the spatial characteristics that amplified POC contributions to beach biogeochemistry, further spatial, temporal, and chemical dynamics may be considered in future studies.

5. Conclusions

Numerical simulations of groundwater flow and reactive transport were used to explore the role of POC in beach biogeochemical reactivity. POC accumulated near the infiltration zone due to retardation along intertidal circulating flow paths. Higher retardation values and a higher tidal amplitude during POC deposition increased the contribution of POC to nitrate removal. Unlike DOC-supported denitrification that occurred along the fringe of the saltwater circulation cell, POC fueled denitrification hot spots landward of the circulation cell. Denitrification supported by POC occurred where anoxic, nitrate-rich water overlapped with POC that was deposited in the beach during antecedent tidal conditions. The ability of the beach aquifer to undergo denitrification depended on the spatial extent of the saline circulation cell, the dynamics of which subsequently controlled the contact between POC and nitrate-rich groundwater. Decreased extent of the circulation cell due to higher freshwater flux from increased hydraulic conductivity increased nitrate removal by allowing greater contact between POC and nitrate-rich groundwater. In contrast, larger circulation cells resulting from higher tidal amplitudes prevented contact between freshwater nitrate and POC, decreasing nitrate removal. In sum, POC within beach sediments, due to their lagged advection, create reaction dynamics that hinge upon the spatial relationship between POC deposition conditions and succeeding hydrologic conditions that control dissolved reactants. The results demonstrate that POC is an important and intermittently utilized reactant that combined with hydrologic dynamics, creates complex, transient reaction patterns within beach aquifers.

Data Availability Statement

Model input and output files for the base case are available on CUAHSI HydroShare (Kim (2020), Modeling hydrologic controls on particulate organic carbon contributions to beach aquifer biogeochemical reactivity, HydroShare, <http://www.hydroshare.org/resource/7e8f77da6bd345ed9bf74c0b7f7c911f>).

Acknowledgments

The authors thank Bill Ullman for his valuable input. This research was funded by NSF EAR-1246554 and EAR-1151733 (to H. M.).

References

- Abarca, E., Karam, H., Hemond, H. F., & Harvey, C. F. (2013). Transient groundwater dynamics in a coastal aquifer: The effects of tides, the lunar cycle, and the beach profile. *Water Resources Research*, 49, 2473–2488. <https://doi.org/10.1029/wrcr.20075>
- Andersen, M. S., Baron, L., Gudbjerg, J., Gregersen, J., Chapellier, D., Jakobsen, R., & Postma, D. (2007). Discharge of nitrate-containing groundwater into a coastal marine environment. *Journal of Hydrology*, 336(1–2), 98–114. <https://doi.org/10.1016/j.jhydrol.2006.12.023>
- Anschutz, P., Smith, T., Mouret, A., Debordé, J., Bujan, S., Poirier, D., & Lecroart, P. (2009). Tidal sands as biogeochemical reactors. *Estuarine, Coastal and Shelf Science*, 84(1), 84–90. <https://doi.org/10.1016/j.ecss.2009.06.015>
- Anwar, N., Robinson, C., & Barry, D. A. (2014). Influence of tides and waves on the fate of nutrients in a nearshore aquifer: Numerical simulations. *Advances in Water Resources*, 73, 203–213. <https://doi.org/10.1016/j.advwatres.2014.08.015>
- Bacon, M. P., Belastock, R. A., & Bothner, M. H. (1994). ^{210}Pb balance and implications for particle transport on the continental shelf, US Middle Atlantic Bight. *Deep Sea Research Part II: Topical Studies in Oceanography*, 41(2–3), 511–535. [https://doi.org/10.1016/0967-0645\(94\)90033-7](https://doi.org/10.1016/0967-0645(94)90033-7)
- Bardini, L., Boano, F., Cardenas, M. B., Revelli, R., & Ridolfi, L. (2012). Nutrient cycling in bedform induced hyporheic zones. *Geochimica et Cosmochimica Acta*, 84, 47–61. <http://doi.org/10.1016/j.gca.2012.01.025>
- Beck, A. J., Tsukamoto, Y., Tovar-Sanchez, A., Huerta-Diaz, M., Bokuniewicz, H. J., & Sanudo-Wilhelmy, S. A. (2007). Importance of geochemical transformations in determining submarine groundwater discharge-derived trace metal and nutrient fluxes. *Applied Geochemistry*, 22(2), 477–490. <https://doi.org/10.1016/j.apgeochem.2006.10.005>
- Beck, M., Reckhardt, A., Amelsberg, J., Bartholomä, A., Brumsack, H., Cypionka, H., et al. (2017). The drivers of biogeochemistry in beach ecosystems: A cross-shore transect from the dunes to the low water line. *Marine Chemistry*, 190, 35–50. <https://doi.org/10.1016/j.marchem.2017.01.001>
- Briggs, M. A., Day-Lewis, F. D., Zarnetske, J. P., & Harvey, J. W. (2015). A physical explanation for the development of redox microzones in hyporheic flow. *Geophysical Research Letters*, 42, 4402–4410. <https://doi.org/10.1002/2015GL064200>
- Burak, S. A., Dogan, E., & Gazioglu, C. (2004). Impact of urbanization and tourism on coastal environment. *Ocean and Coastal Management*, 47(9–10), 515–527. <https://doi.org/10.1016/j.ocecoaman.2004.07.007>
- Carter, R. W. G. (1988). *Coastal Environments: An Introduction to the Physical, Ecological, and Cultural Systems of Coastlines*. London: Academic Press Limited.
- Chailou, G., Lemay-Borduas, F., & Couturier, M. (2016). Transport and transformations of groundwater-borne carbon discharging through a sandy beach to a coastal ocean. *Canadian Water Resources Journal*, 41(4), 455–468. <https://doi.org/10.1080/07011784.2015.1111775>
- Charbonnier, C., Anschutz, P., Poirier, D., Bujan, S., & Lecroart, P. (2013). Aerobic respiration in a high-energy sandy beach. *Marine Chemistry*, 155, 10–21. <https://doi.org/10.1016/j.marchem.2013.05.003>
- Charette, M. A., & Sholkovitz, E. R. (2002). Oxidative precipitation of groundwater-derived ferrous iron in the subterranean estuary of a coastal bay. *Geophysical Research Letters*, 29(10), 1444. <https://doi.org/10.1029/2001GL014512>
- Charette, M. A., Sholkovitzand, E. R., & Hansel, C. M. (2005). Trace element cycling in a subterranean estuary: Part 1. Geochemistry of the permeable sediments. *Geochimica et Cosmochimica Acta*, 69(8), 2095–2109. <https://doi.org/10.1016/j.gca.2004.10.024>
- Cloern, J. E. (2001). Our evolving conceptual model of the coastal eutrophication problem. *Marine Ecology Progress Series*, 210, 223–253. <https://doi.org/10.3354/meps210223>
- Costanza, R., d'Arge, R., de Groot, R., Farber, S., Grasso, M., Hannon, B., et al. (1997). The value of the world's ecosystem services and natural capital. *Nature*, 387(6630), 253–260. <https://doi.org/10.1038/387253a0>
- Couturier, M., Nozaïs, C., & Chaillou, G. (2016). Microtidal subterranean estuaries as a source of fresh terrestrial dissolved organic matter to the coastal ocean. *Marine Chemistry*, 186, 46–57. <https://doi.org/10.1016/j.marchem.2016.08.001>
- Davis, H. (2000). Fate and transport modeling of selected chlorinated organic compounds at operable unit 3, US naval Air Station, Jacksonville, Florida, Department of the Interior, Washington D.C., USGS-OFR-00-255, <https://apps.dtic.mil/dtic/tr/fulltext/u2/a442391.pdf>
- Diaz, R. J., & Solow, A. (1999). *Ecological and Economic Consequences of Hypoxia*. Silver Spring, Maryland: NOAA Coastal Ocean Program.
- Doney, S. C. (2010). The growing human footprint on coastal and open-ocean biogeochemistry. *Science*, 328(5985), 1512–1516. <https://doi.org/10.1126/science.1185198>
- El-Farhan, Y. H., DeNovio, N. M., Herman, J. S., & Hornberger, G. M. (2000). Mobilization and transport of soil particles during infiltration experiments in an agricultural field, Shenandoah Valley, Virginia. *Environmental Science & Technology*, 34(17), 3555–3559. <https://doi.org/10.1021/es991099g>
- Gast, R. J., Elgar, S., & Raubenheimer, B. (2015). Observations of transport of bacterial-like microspheres through beach sand. *Continental Shelf Research*, 97, 1–6. <https://doi.org/10.1016/j.csr.2015.01.010>
- Gelhar, L. W., Welty, C., & Rehfeldt, K. R. (1992). A critical review of data on field-scale dispersion in aquifers. *Water Resources Research*, 28(7), 1955–1974. <https://doi.org/10.1029/92WR00607>
- Gu, C. H., Hornberger, G. M., Mills, A. L., Herman, J. S., & Flewelling, S. A. (2007). Nitrate reduction in streambed sediments: Effects of flow and bio-geochemical kinetics. *Water Resources Research*, 43, W12413. <https://doi.org/10.1029/2007WR006027>
- Hays, R. L., & Ullman, W. J. (2007). Direct determination of total and fresh groundwater discharge and nutrient loads from a sandy beachface at low tide (Cape Henlopen, Delaware). *Limnology and Oceanography*, 52(1), 240–247. <https://doi.org/10.4319/lo.2007.52.1.0240>
- Heiss, J. W. (2020). Whale burial and organic matter impacts on biogeochemical cycling in beach aquifers and leachate fluxes to the nearshore zone. *Journal of Contaminant Hydrology*, 233, 103656. <https://doi.org/10.1016/j.jconhyd.2020.103656>
- Heiss, J. W., & Michael, H. A. (2014). Saltwater-freshwater mixing dynamics in a sandy beach aquifer over tidal, spring-neap, and seasonal cycles. *Water Resources Research*, 50, 6747–6766. <https://doi.org/10.1002/2014WR015574>
- Heiss, J. W., Michael, H. A., & Koneshloo, M. (2020). Denitrification hotspots in intertidal mixing zones linked to geologic heterogeneity. *Environmental Research Letters*, 15(8), 084015. <https://doi.org/10.1088/1748-9326/ab90a6>
- Heiss, J. W., Post, V. E., Laatto, T., Russoniello, C. J., & Michael, H. A. (2017). Physical controls on biogeochemical processes in intertidal zones of beach aquifers. *Water Resources Research*, 53, 9225–9244. <https://doi.org/10.1002/2017WR021110>
- Huettel, M., Berg, P., & Kostka, J. E. (2014). Benthic exchange and biogeochemical cycling in permeable sediments. *Annual Review of Marine Science*, 6(1), 23–51. <https://doi.org/10.1146/annurev-marine-051413-012706>
- Huettel, M., & Rusch, A. (2000). Transport and degradation of phytoplankton in permeable sediment. *Limnology and Oceanography*, 45(3), 534–549. <https://doi.org/10.4319/lo.2000.45.3.0534>

- Jiao, L., Wu, J., He, X., Wen, X., Li, Y., & Hong, Y. (2018). Significant microbial nitrogen loss from denitrification and anammox in the land-sea interface of low permeable sediments. *International Biodeterioration & Biodegradation*, 135, 80–89. <https://doi.org/10.1016/j.ibiod.2018.10.002>
- Johannes, R. E. (1980). Ecological significance of the submarine discharge of groundwater. *Marine Ecology Progress Series*, 3(4), 365–373. <https://doi.org/10.3354/meps003365>
- Kim, K. H. (2020). Modeling Hydrologic Controls on Particulate Organic Carbon Contributions to Beach Aquifer Biogeochemical Reactivity, HydroShare, <http://www.hydroshare.org/resource/7e8f77da6bd345ed9bf74c0b7f7c911f>
- Kim, K. H., Heiss, J. W., Michael, H. A., Cai, W. J., Laattoe, T., Post, V. E., & Ullman, W. J. (2017). Spatial patterns of groundwater biogeochemical reactivity in an intertidal beach aquifer. *Journal of Geophysical Research: Biogeosciences*, 122, 2548–2562. <https://doi.org/10.1002/2017JG003943>
- Kim, K. H., Michael, H. A., Field, E. K., & Ullman, W. J. (2019). Hydrologic shifts create complex transient distributions of particulate organic carbon and biogeochemical responses in beach aquifers. *Journal of Geophysical Research: Biogeosciences*, 124, 3024–3038. <https://doi.org/10.1029/2019JG005114>
- Kim, T. H., Kwon, E., Kim, I., Lee, S. A., & Kim, G. (2013). Dissolved organic matter in the subterranean estuary of a volcanic island, Jeju: Importance of dissolved organic nitrogen fluxes to the ocean. *Journal of Sea Research*, 78, 18–24. <https://doi.org/10.1016/j.seares.2012.12.009>
- Kim, T. H., Waska, H., Kwon, E., Suryaputra, I. G. N., & Kim, G. (2012). Production, degradation, and flux of dissolved organic matter in the subterranean estuary of a large tidal flat. *Marine Chemistry*, 142–144, 1–10. <https://doi.org/10.1016/j.marchem.2012.08.002>
- Kroeger, K. D., & Charette, M. A. (2008). Nitrogen biogeochemistry of submarine groundwater discharge. *Limnology and Oceanography*, 53(3), 1025–1039. <https://doi.org/10.4319/lo.2008.53.3.1025>
- Kroeger, K. D., Cole, M. L., & Valiela, I. (2006). Groundwater-transported dissolved organic nitrogen exports from coastal watersheds. *Limnology and Oceanography*, 51(5), 2248–2261. <https://doi.org/10.4319/lo.2006.51.5.2248>
- Krupka, K. M., Kaplan, D. I., Whelan, G., Serne, R. J., & Mattigod, S. V. (1999). *Understanding Variation in Partition Coefficient, Kd, Values, Volume II: Review of Geochemistry and Available Kd Values for Cadmium, Cesium, Chromium, Lead, Plutonium, Radon, Strontium, Thorium, Tritium (3H), and Uranium*. Washington D.C: EPA. <https://www.epa.gov/sites/production/files/2015-05/documents/402-r-99-004b.pdf>
- Kuan, W. K., Jin, G., Xin, P., Robinson, C., Gibbes, B., & Li, L. (2012). Tidal influence on seawater intrusion in unconfined coastal aquifers. *Water Resources Research*, 48, W02502. <https://doi.org/10.1029/2011WR010678>
- Lamontagne, S., Cosme, F., Minard, A., & Holloway, A. (2018). Nitrogen attenuation, dilution and recycling in the intertidal hyporheic zone of a subtropical estuary. *Hydrology and Earth System Sciences*, 22(7), 4083–4096. <https://doi.org/10.5194/hess-22-4083-2018>
- Langevin, C. D., & Guo, W. (2006). MODFLOW/MT3DMS-based simulation of variable-density ground water flow and transport. *Groundwater*, 44(3), 339–351. <https://doi.org/10.1111/j.1745-6584.2005.00156.x>
- Langevin, C. D., Thorne, D. T., Dausman, A. M., Sukop, M. C., & Guo, W. (2007). SEAWAT Version 4: A Computer Program for Simulation of Multi-Species Solute and Heat Transport (Technical Report, U.S. Geological Survey Techniques and Methods Book 6, Chapter A22, 39 Pp.). Reston, VA: U.S. Geological Survey.
- Martínez, M. L., Intralawan, A., Vázquez, G., Pérez-Maqueo, O., Sutton, P., & Landgrave, R. (2007). The coasts of our world: Ecological, economic and social importance. *Ecological Economics*, 63(2–3), 254–272. <https://doi.org/10.1016/j.ecolecon.2006.10.022>
- McAllister, S. M., Barnett, J. M., Heiss, J. W., Findlay, A. J., MacDonald, D. J., Dow, C. L., et al. (2015). Dynamic hydrologic and biogeochemical processes drive microbially enhanced iron and sulfur cycling within the intertidal mixing zone of a beach aquifer. *Limnology and Oceanography*, 60(1), 329–345. <https://doi.org/10.1111/lio.10029>
- McDowell-Boyer, L. M., Hunt, J. R., & Sitar, N. (1986). Particle transport through porous media. *Water Resources Research*, 22(13), 1901–1921. <https://doi.org/10.1029/WR022i013p01901>
- McLachlan, A., Eliot, I. G., & Clarke, D. J. (1985). Water filtration through reflective microtidal beaches and shallow sublittoral sands and its implications for an inshore ecosystem in Western Australia, Estuarine. *Coastal and Shelf Science*, 21(1), 91–104. [https://doi.org/10.1016/0272-7714\(85\)90008-3](https://doi.org/10.1016/0272-7714(85)90008-3)
- Michael, H. A., Mulligan, A. E., & Harvey, C. F. (2005). Seasonal oscillations in water exchange between aquifers and the coastal ocean. *Nature*, 436(7054), 1145–1148. <https://doi.org/10.1038/nature03935>
- Michael, H. A., Post, V. E. A., Wilson, A. M., & Werner, A. D. (2017). Science, society, and the coastal groundwater squeeze. *Water Resources Research*, 53, 2610–2617. <https://doi.org/10.1029/2017WR020851>
- Moore, W. S. (1999). The subterranean estuary: A reaction zone of ground water and sea water. *Marine Chemistry*, 65(1–2), 111–125. [https://doi.org/10.1016/S0304-4203\(99\)00014-6](https://doi.org/10.1016/S0304-4203(99)00014-6)
- Ocampo, C. J., Oldham, C. E., & Sivapalan, M. (2006). Nitrate attenuation in agricultural catchments: Shifting balances between transport and reaction. *Water Resources Research*, 42, W01408. <https://doi.org/10.1029/2004WR003773>
- O'Connor, A. E., Krask, J. L., Canuel, E. A., & Beck, A. J. (2018). Seasonality of major redox constituents in a shallow subterranean estuary. *Geochimica et Cosmochimica Acta*, 224, 344–361. <https://doi.org/10.1016/j.gca.2017.10.013>
- Oh, Y. H., Lee, Y. W., Park, S. R., & Kim, T. H. (2017). Importance of dissolved organic carbon flux through submarine groundwater discharge to the coastal ocean: Results from Masan Bay, the southern coast of Korea. *Journal of Marine Systems*, 173, 43–48. <https://doi.org/10.1016/j.jmarsys.2017.03.013>
- Orr, M., Zimmer, M., Jelinski, D. E., & Mews, M. (2005). Wrack deposition on different beach types: Spatial and temporal variation in the pattern of subsidy. *Ecology*, 86(6), 1496–1507. <https://doi.org/10.1890/04-1486>
- Pilditch, C. A., & Miller, D. C. (2006). Phytoplankton deposition to permeable sediments under oscillatory flow: Effects of ripple geometry and resuspension. *Continental Shelf Research*, 26(15), 1806–1825. <https://doi.org/10.1016/j.csr.2006.06.002>
- Post, V. E. A. (2011). A new package for simulating periodic boundary conditions in MODFLOW and SEAWAT. *Computers & Geosciences*, 37(11), 1843–1849.
- Prommer, H., & Post, V. (2002). *A Reactive Multicomponent Transport Model for Saturated Porous Media*. Edinburgh, UK: Contaminated Land Assessment and Remediation Research Centre, The University of Edinburgh.
- Pronk, M., Goldscheider, N., Zopfi, J., & Zwahlen, F. (2009). Percolation and particle transport in the unsaturated zone of a karst aquifer. *Groundwater*, 47(3), 361–369. <https://doi.org/10.1111/j.1745-6584.2008.00509.x>
- Reckhardt, A., Beck, M., Seidel, M., Riedel, T., Wehrmann, A., Bartholomä, A., & Brumsack, H. J. (2015). Carbon, nutrient and trace metal cycling in sandy sediments: A comparison of high-energy beaches and backbarrier tidal flats. *Estuarine, Coastal and Shelf Science*, 159, 1–14. <https://doi.org/10.1016/j.ecss.2015.03.025>

- Robinson, C., Gibbes, B., Carey, H., & Li, L. (2007). Salt-freshwater dynamics in a subterranean estuary over a spring-neap tidal cycle. *Journal of Geophysical Research*, 112, C09007. <https://doi.org/10.1029/2006JC003888>
- Robinson, C., Gibbes, B., & Li, L. (2006). Driving mechanisms for groundwater flow and salt transport in a subterranean estuary. *Geophysical Research Letters*, 33, L03402. <https://doi.org/10.1029/2005GL025247>
- Rocha, C., Forster, S., Koning, E., & Epping, E. (2005). High-resolution permeability determination and two-dimensional porewater flow in sandy sediment. *Limnology and Oceanography: Methods*, 3(1), 10–23. <https://doi.org/10.4319/lom.2005.3.10>
- Roy, M., Martin, J. B., Cable, J. E., & Smith, C. G. (2013). Variations of iron flux and organic carbon remineralization in a subterranean estuary caused by inter-annual variations in recharge. *Geochimica et Cosmochimica Acta*, 103, 301–315. <https://doi.org/10.1016/j.gca.2012.10.055>
- Roy, M., Martin, J. B., Cherrier, J., Cable, J. E., & Smith, C. G. (2010). Influence of sea level rise on iron diagenesis in an east Florida subterranean estuary. *Geochimica et Cosmochimica Acta*, 74(19), 5560–5573. <https://doi.org/10.1016/j.gca.2010.07.007>
- Rusch, A., & Huettel, M. (2000). Advective particle transport into permeable sediments—Evidence from experiments in an intertidal sandflat. *Limnology and Oceanography*, 45(3), 525–533. <https://doi.org/10.4319/lo.2000.45.3.00525>
- Rusch, A., Huettel, M., & Forster, S. (2000). Particulate organic matter in permeable marine sands—Dynamics in time and depth, estuarine. *Coastal and Shelf Science*, 51(4), 399–414. <https://doi.org/10.1006/ecss.2000.0687>
- Sawyer, A. H. (2015). Enhanced removal of groundwater-borne nitrate in heterogeneous aquatic sediments. *Geophysical Research Letters*, 42, 403–410. <https://doi.org/10.1002/2014GL062234>
- Seidel, M., Beck, M., Greskowiak, J., Riedel, T., Waska, H., Suryaputra, I. G. N. A., et al. (2015). Benthic-pelagic coupling of nutrients and dissolved organic matter composition in an intertidal sandy beach. *Marine Chemistry*, 176, 150–163. <https://doi.org/10.1016/j.marchem.2015.08.011>
- Seidel, M., Beck, M., Riedel, T., Waska, H., Suryaputra, I. G., Schnetger, B., et al. (2014). Biogeochemistry of dissolved organic matter in an anoxic intertidal creek bank. *Geochimica et Cosmochimica Acta*, 140, 418–434. <https://doi.org/10.1016/j.gca.2014.05.038>
- Slomp, C. P., & Van Cappellen, P. (2004). Nutrient inputs to the coastal ocean through submarine groundwater discharge: Controls and potential impact. *Journal of Hydrology*, 295(1–4), 64–86. <https://doi.org/10.1016/j.jhydrol.2004.02.018>
- Spiteri, C., Slomp, C. P., Charette, M. A., Tuncay, K., & Meile, C. (2008). Flow and nutrient dynamics in a subterranean estuary (Waquoit Bay, MA, USA): Field data and reactive transport modeling. *Geochimica et Cosmochimica Acta*, 72(14), 3398–3412. <https://doi.org/10.1016/j.gca.2008.04.027>
- Spiteri, C., Slomp, C. P., Tuncay, K., & Meile, C. (2008). Modeling biogeochemical processes in subterranean estuaries: Effect of flow dynamics and redox conditions on submarine groundwater discharge of nutrients. *Water Resources Research*, 44, W02430. <https://doi.org/10.1029/2007WR006071>
- Ullman, W. J., Chang, B., Miller, D. C., & Madsen, J. A. (2003). Groundwater mixing, nutrient diagenesis, and discharges across a sandy beachface, Cape Henlopen, Delaware (USA), Estuarine. *Coastal and Shelf Science*, 57(3), 539–552. [https://doi.org/10.1016/S0272-7714\(02\)00398-0](https://doi.org/10.1016/S0272-7714(02)00398-0)
- van der Meulen, F., Bakker, T. W. M., & Houston, J. A. (2004). The costs of our coasts: Examples of dynamic dune management from Western Europe. In *Coastal Dunes: Ecology and Conservation* (pp. 259–278). Berlin: Springer-Verlag.
- Valiela, I., Costa, J., Foreman, K., Teal, J. M., Howes, B., & Aubrey, D. (1990). Transport of groundwater-borne nutrients from watersheds and their effects on coastal waters. *Biogeochemistry*, 10, 177–197.
- Vandenbohede, A., & Lebbe, L. (2006). Occurrence of salt water above fresh water in dynamic equilibrium in a coastal groundwater flow system near De Panne, Belgium. *Hydrogeology Journal*, 14(4), 462–472. <https://doi.org/10.1007/s10040-005-0446-5>
- Vitousek, P. M., Aber, J. D., Howarth, R. W., Likens, G. E., Matson, P. A., Schindler, D. W., et al. (1997). Human alteration of the global nitrogen cycle: Sources and consequences. *Ecological Applications*, 7(3), 737–750. [https://doi.org/10.1890/1051-0761\(1997\)007\[0737:HAOTGN\]2.0.CO;2](https://doi.org/10.1890/1051-0761(1997)007[0737:HAOTGN]2.0.CO;2)
- Wang, Y., & Van Cappellen, P. (1996). A multicomponent reactive transport model of early diagenesis: Application to redox cycling in coastal marine sediments. *Geochimica et Cosmochimica Acta*, 60(16), 2993–3014.
- Zarnetske, J. P., Haggerty, R., Wondzell, S. M., Bokil, V. A., & González-Pinzón, R. (2012). Coupled transport and reaction kinetics control the nitrate source-sink function of hyporheic zones. *Water Resources Research*, 48, W11508. <https://doi.org/10.1029/2012WR011894>